

## Comparison of Atmospheric Pressure Chemical Ionization and Field Ionization Mass Spectrometry for the Analysis of Large Saturated Hydrocarbons

Chunfen Jin<sup>a,b</sup>, Jyrki Viidanoja<sup>\*,b</sup>, Mingzhe Li<sup>a</sup>, Yuyang Zhang<sup>a</sup>, Elias Ikonen<sup>b</sup>, Andrew Root<sup>c</sup>, Mark Romanczyk<sup>a</sup>, Jeremy Manheim<sup>a</sup>, Eric Dziekonski<sup>a</sup>, Hilkka I. Kenttämä<sup>\*,a</sup>

<sup>a</sup>Department of Chemistry, Purdue University, West Lafayette, Indiana 47907, United States

<sup>b</sup>Technology Centre, Neste Corporation, P.O. Box 310, FI-06101 Porvoo, Finland

<sup>c</sup>MagSol, Tuhkanummenkuja 2, FI-00970 Helsinki, Finland

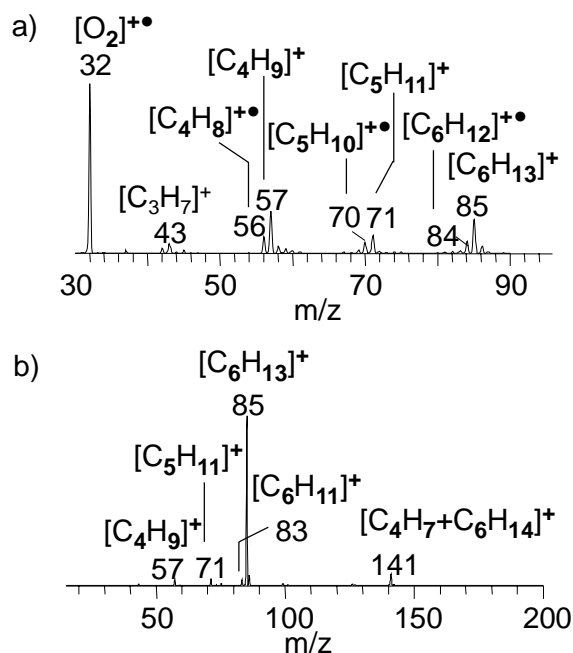
\*Professor Hilkka I. Kenttämä. E-mail: [hilkka@purdue.edu](mailto:hilkka@purdue.edu)

\*Dr Jyrki Viidanoja. E-mail: [jyrki.viidanoja@neste.com](mailto:jyrki.viidanoja@neste.com)

Table of Contents	Pages
Ion-molecule Reaction Studies.....	S-3
Scheme S1. Possible pathways for the formation of $[M-H]^+$ ions for saturated hydrocarbons (M) in hexane upon APCI using oxygen as the ion source gas .....	S-4
Figure S1. A mass spectrum measured after reactions of $[O_2]^+\bullet$ with hexane within the ion trap for 500 ms. Positive ion mode APCI mass spectrum of hexane with $O_2$ as the ion source gas.....	S-3
Figure S2. Mass spectra measured after reactions of butylcyclohexane with $[O_2]^+\bullet$ in the ion trap, and with $[C_4H_9]^+$ in the ion trap.....	S-4
Figure S3. Direct infusion positive ion mode low-resolution APCI mass spectra of the low viscosity lubricant base oil in hexane obtained using LQIT/Orbitrap and nitrogen or oxygen as the ion source gas, and a zoomed view of the mass region $m/z$ 240 - 270 of a high-resolution mass spectrum measured by using the Orbitrap mass spectrometer with oxygen as the ion source gas.....	S-5
Figure S4. Three examples of positive ion mode FI mass spectra measured for low viscosity lubricant base oil .....	S-6
Figure S5. Three examples of positive ion mode FI mass spectra measured for middle viscosity lubricant base oil .....	S-7
Figure S6. Three examples of positive ion mode FI mass spectra measured for high viscosity lubricant base oil .....	S-8
Figure S7. Positive ion mode FI mass spectrum of squalane determined using a brand new FI emitter.....	S-9
Figure S8. Hydrocarbon type distributions as a function of carbon number determined for low viscosity base oil by using APCI-MS and FI-MS.....	S-10
Figure S9. Hydrocarbon type distributions as a function of carbon number determined for middle viscosity base oil by using APCI-MS and FI-MS.....	S-11
Figure S10. Hydrocarbon type distributions as a function of carbon number determined for high viscosity base oil by using APCI-MS and FI-MS.....	S-12
Figure S11. Naphthenic structures, their carbon numbers and relative contributions used to calculate average amounts of naphthenic carbons.....	S-13

**Ion-Molecule Reaction Studies.** Possible mechanisms for the formation of the  $[M-H]^+$  ions upon APCI were investigated in more detail by performing ion-molecule reactions under controlled conditions within the ion trap of LQIT. Two volatile hydrocarbons were introduced individually into the ion trap via a pulsed valve. The compounds were hexane (used as a solvent in all APCI studies discussed above) and n-butylcyclohexane. The latter compound was selected because it resembles alkylnaphthenes and is volatile enough to be introduced into the ion trap via the pulsed valve. Reagent ions,  $[O_2]^{+\bullet}$  (m/z 32),  $[C_6H_{13}]^+$  (m/z 85),  $[C_6H_{11}]^+$  (m/z 83),  $[C_5H_{11}]^+$  (m/z 71),  $[C_4H_9]^+$  (m/z 57), and  $[C_6H_{14}]$  (m/z 141), generated upon APCI from oxygen or hexane, were introduced into the ion trap, isolated and allowed to react with the hydrocarbons for 500 ms.

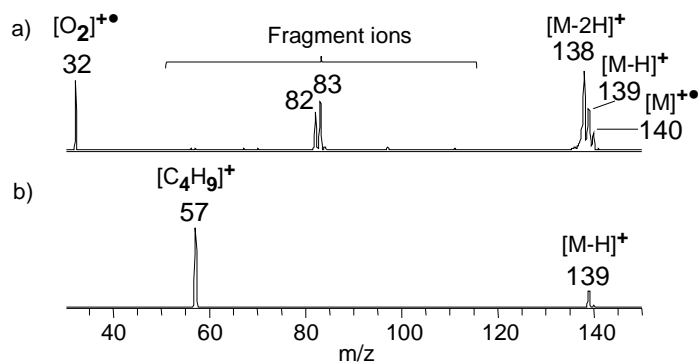
Reactions of  $[O_2]^{+\bullet}$  with hexane at low pressure within the ion trap resulted in generation of some molecular and pseudo-molecular ions as well as a significant amount of fragment ions (Figure S1a). In contrast, direct infusion of hexane into the APCI source using oxygen as the ion source gas (Figure S1b) yielded predominantly  $[C_6H_{13}]^+$  ( $[M-H]^+$ ) ions with a small amount of  $[C_4H_9]^+$  (m/z 57),  $[C_5H_{11}]^+$  (m/z 71) and  $[C_6H_{11}]^+$  (m/z 83) fragment ions and  $[C_4H_7+C_6H_{14}]^+$  (m/z 141) adduct ions. These results suggest that either 1) the fragment ions of hexane are consumed quicker than  $[M-H]^+$  ions at the atmospheric pressure than at low pressure, or 2) the conditions at atmospheric pressure favor formation of  $[M-H]^+$  ions over the fragment ions.



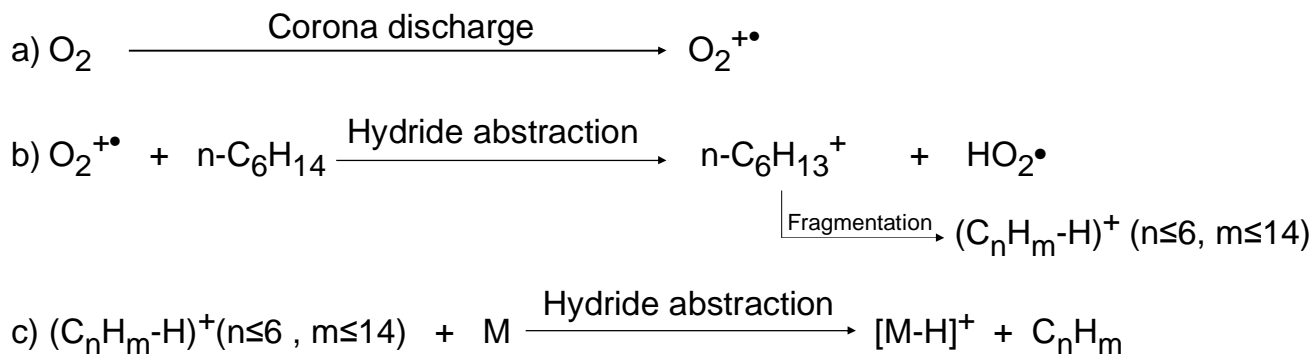
**Figure S1.** a) A mass spectrum measured after reactions of  $[O_2]^{+\bullet}$  (generated upon APCI) with hexane (MW 86) within the ion trap for 500 ms. Both even-electron carbocations and radical cations derived from hexane were observed. b) Positive ion mode APCI mass spectrum of hexane with  $O_2$  as the ion source gas. Only even-electron carbocations derived from hexane were observed.

## SUPPORTING INFORMATION

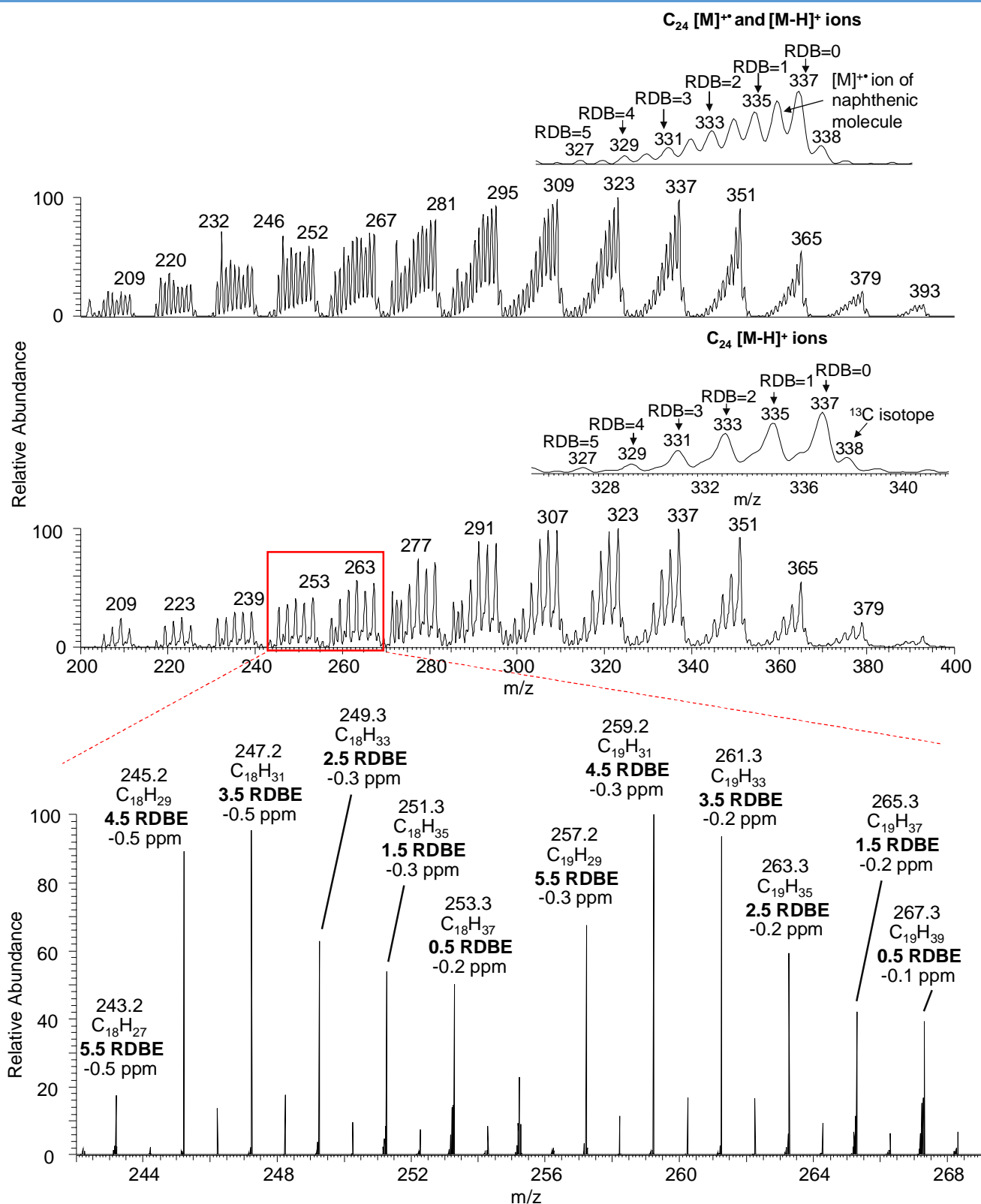
Reactions of  $[\text{O}_2]^{+\bullet}$  with butylcyclohexane (M) in the ion trap formed  $[\text{M}]^{+\bullet}$ ,  $[\text{M}-2\text{H}]^{+\bullet}$  and  $[\text{M}-\text{H}]^+$  ions as well as abundant fragment ions (Figure S2a). However, reactions of carbocations of m/z 57 (derived from hexane) with butylcyclohexane within the ion trap produced only  $[\text{M}-\text{H}]^+$  ions via hydride abstraction with no fragmentation (Figure S2b). The rest of the reagent ions,  $[\text{C}_5\text{H}_{11}]^+$  (m/z 71),  $[\text{C}_6\text{H}_{11}]^+$  (m/z 83), and  $[\text{C}_6\text{H}_{13}]^+$  (m/z 85), provided the same results as the reagent ion  $[\text{C}_4\text{H}_9]^+$  (m/z 57, Figure S2b). Above results demonstrate that large saturated hydrocarbons can be ionized by hydride abstraction without fragmentation in the ion trap if the reagent ion is one of the above carbocations derived from hexane. However, if the reagent ion is  $[\text{O}_2]^{+\bullet}$ , this is not the case. The same may be true for APCI. A possible pathway for the formation of  $[\text{M}-\text{H}]^+$  ions from a hydrocarbon (M) in hexane upon atmospheric pressure chemical ionization with oxygen ion source gas is shown in Scheme S1. Oxygen was selected for Scheme S1 instead of nitrogen because oxygen was used as the ion source gas in the final APCI method in this study.



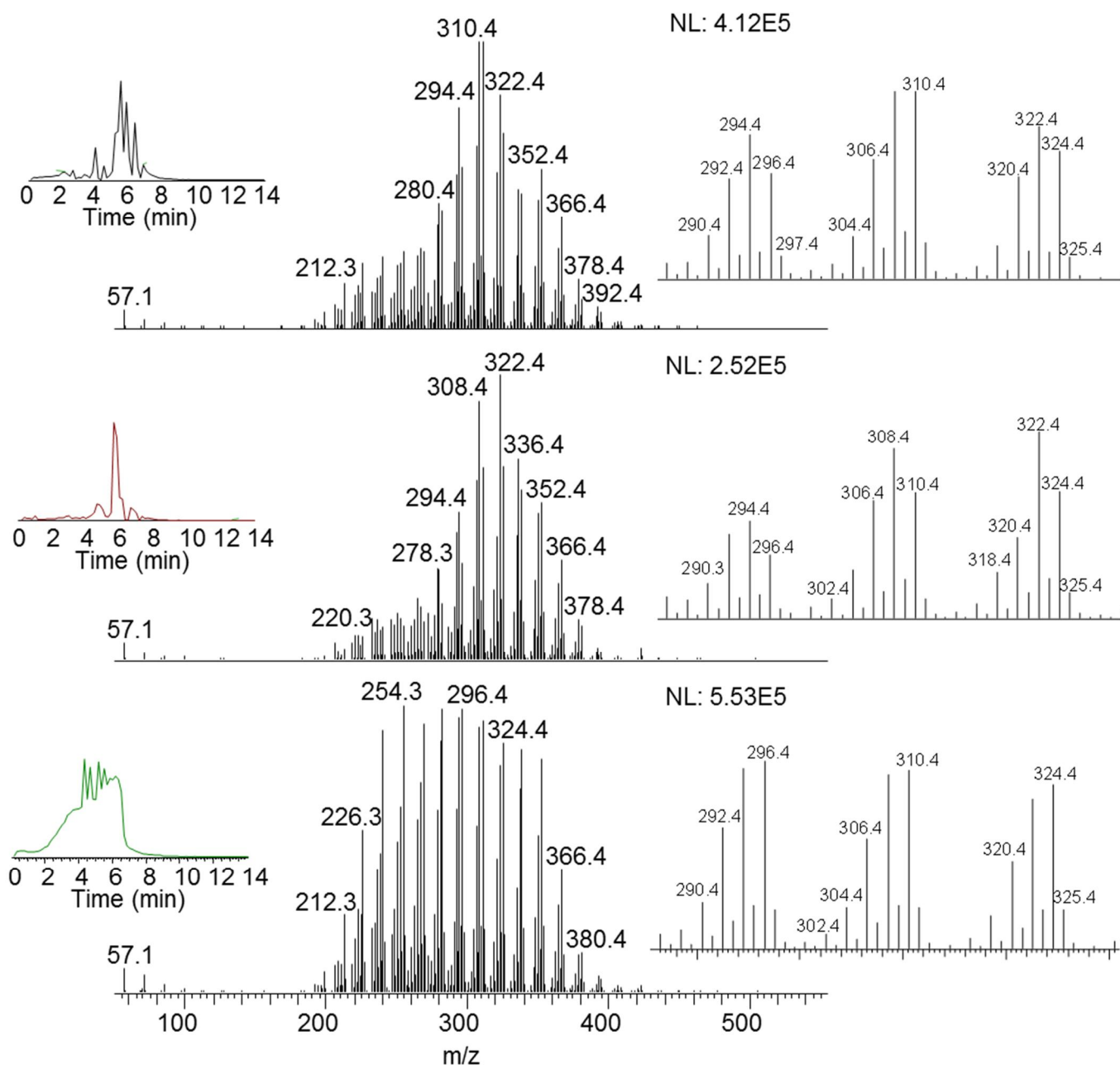
**Figure S2.** Mass spectra measured after reactions of butylcyclohexane (M; MW 140) with a)  $[\text{O}_2]^{+\bullet}$  (generated upon APCI) in the ion trap, and b)  $[\text{C}_4\text{H}_9]^+$  (m/z 57; generated upon APCI using oxygen as ion source gas and hexane as reagent) in the ion trap.



**Scheme S1.** Possible pathways for the formation of  $[\text{M}-\text{H}]^+$  ions for saturated hydrocarbons (M) in hexane upon APCI using oxygen as the ion source gas: a) ionization of oxygen, b) ionization of hexane, and c) ionization of an analyte.  $(\text{C}_n\text{H}_m\text{-H})^+$  ( $n \leq 6, m \leq 14$ ) indicates the carbocation fragments derived from hexane.

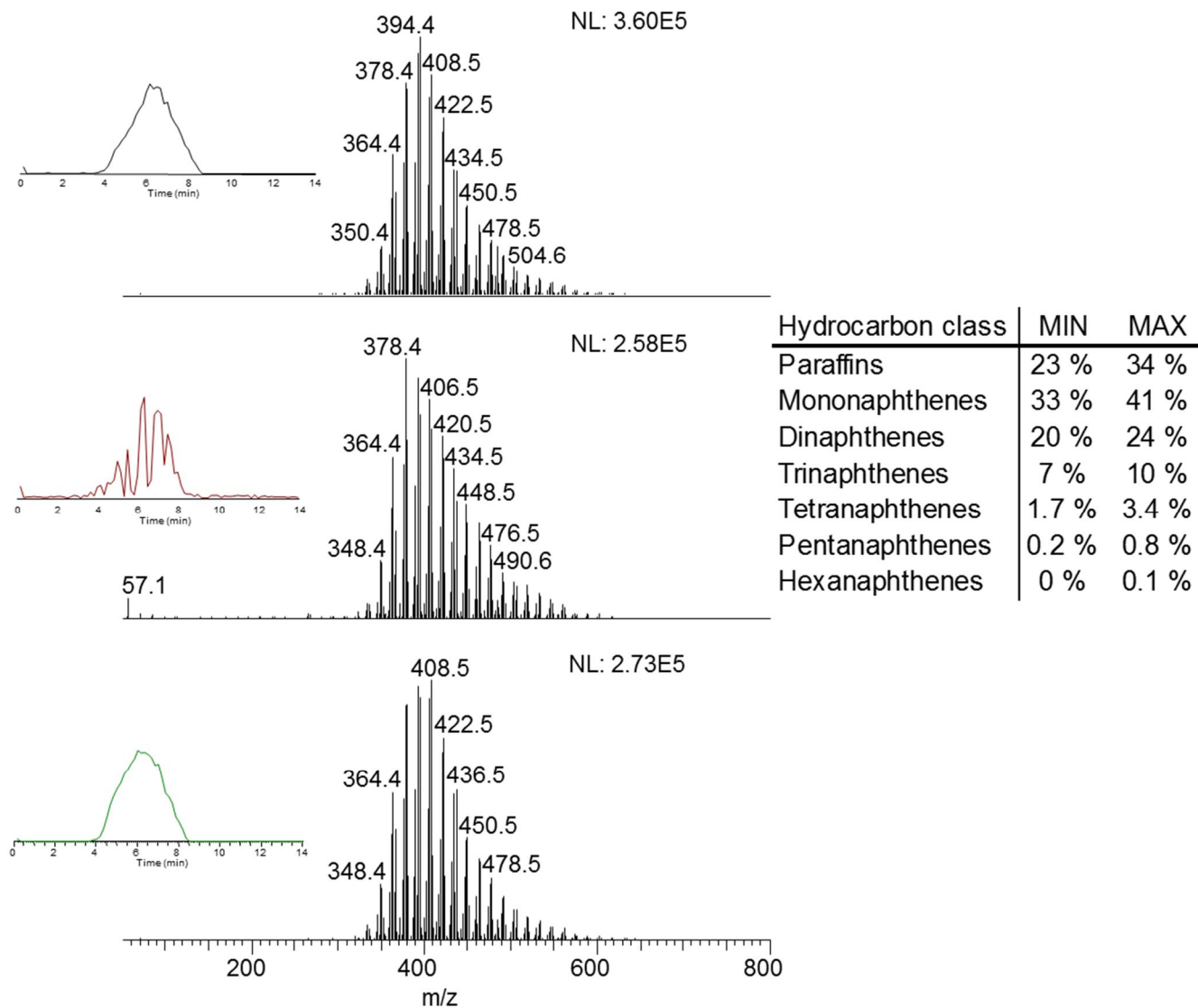


**Figure S3.** Direct infusion positive ion mode low-resolution APCI mass spectra of the low viscosity lubricant base oil in hexane obtained using LQIT/Orbitrap and nitrogen (top) or oxygen (middle) as the ion source gas, and a zoomed view of the mass region  $m/z$  240 - 270 of a high-resolution mass spectrum (bottom) measured by using the Orbitrap mass spectrometer with oxygen as the ion source gas.



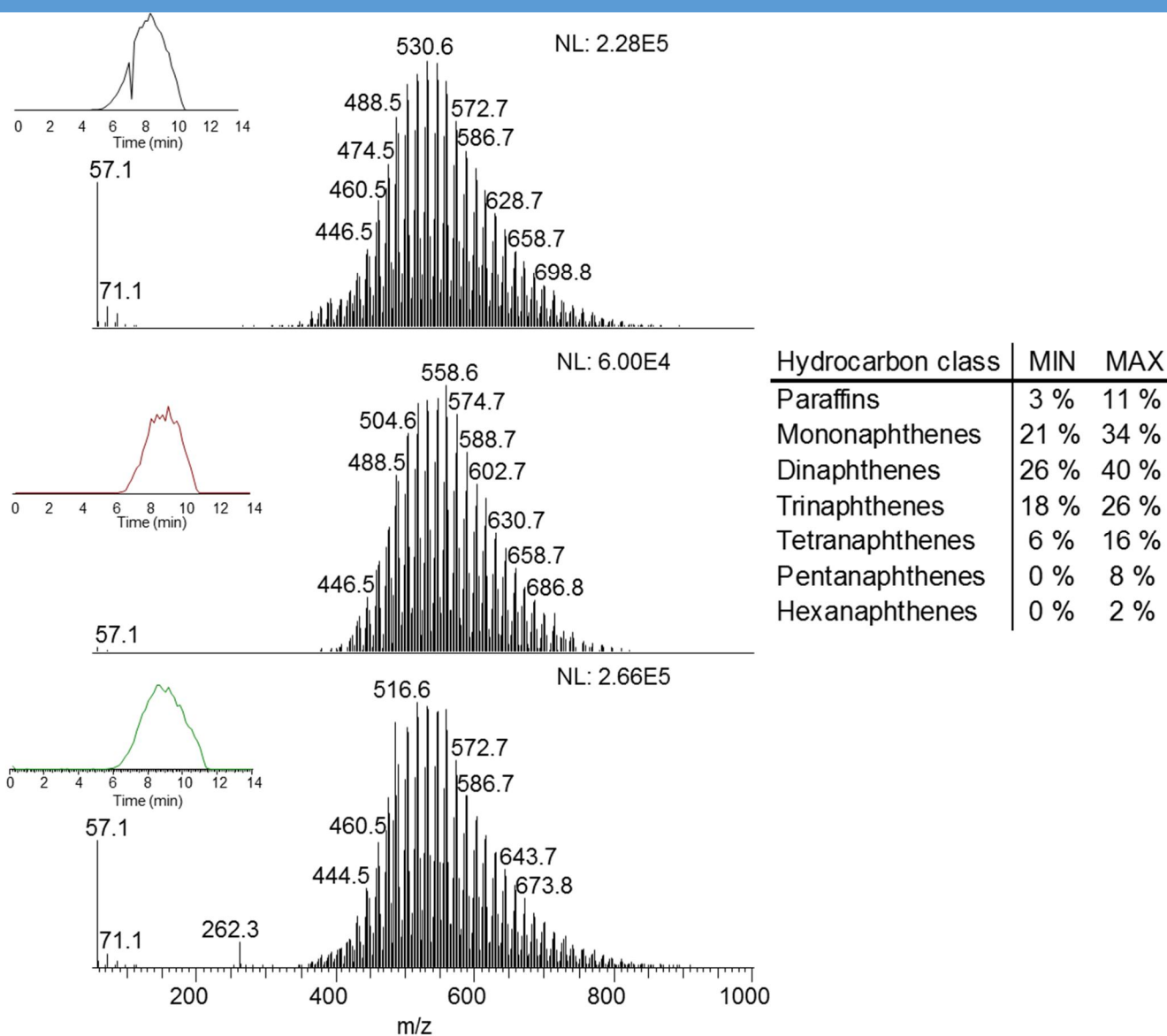
**Figure S4.** Three examples of positive ion mode FI mass spectra measured for the low viscosity lubricant base oil. The spectra represent typical variation of ion distributions within and between days. Total ion current as a function of acquisition time is shown on the left. Zoom view of the mass spectrum for a selected mass range of  $m/z$  285-330 is shown on the right.

## SUPPORTING INFORMATION



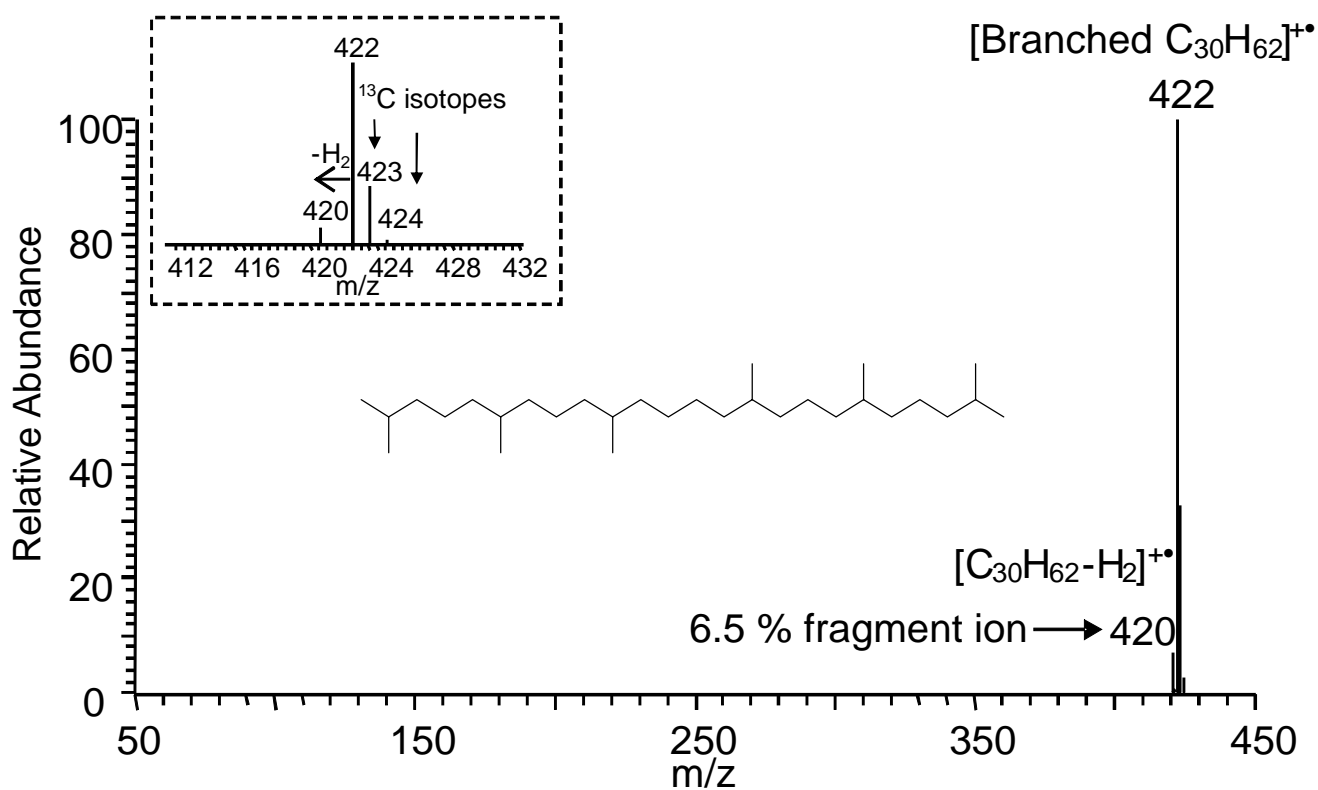
**Figure S5.** Three examples of positive ion mode FI mass spectra measured for the middle viscosity lubricant base oil. The spectra represent typical variation of ion distributions within and between days. Total ion current as a function of acquisition time is shown on the left. Variation of the hydrocarbon class distribution (wt %) of the middle viscosity base oil, based on six measurement days, three replicates per day, is shown on the right.

## SUPPORTING INFORMATION

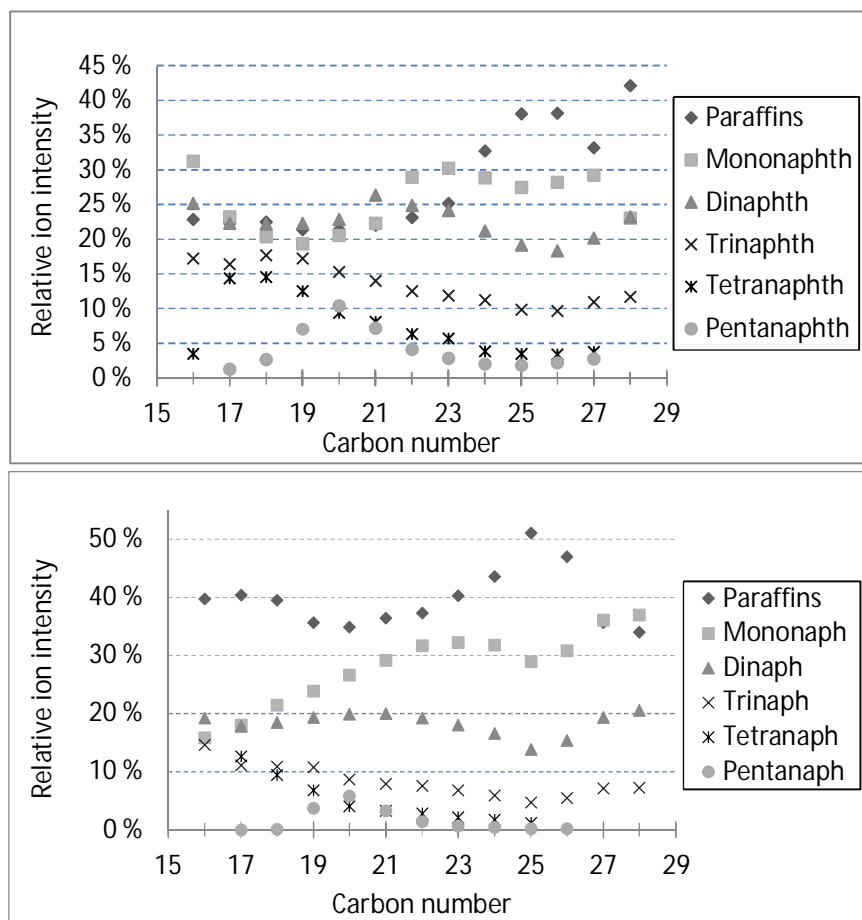


**Figure S6.** Three examples of positive ion mode FI mass spectra measured for the high viscosity lubricant base oil. The spectra represent typical variation of ion distributions within and between days. Total ion current as a function of acquisition time is shown on the left. Variation of the hydrocarbon class distribution (wt %) of the high viscosity base oil, based on six measurement days, three replicates per day, is shown on the right.

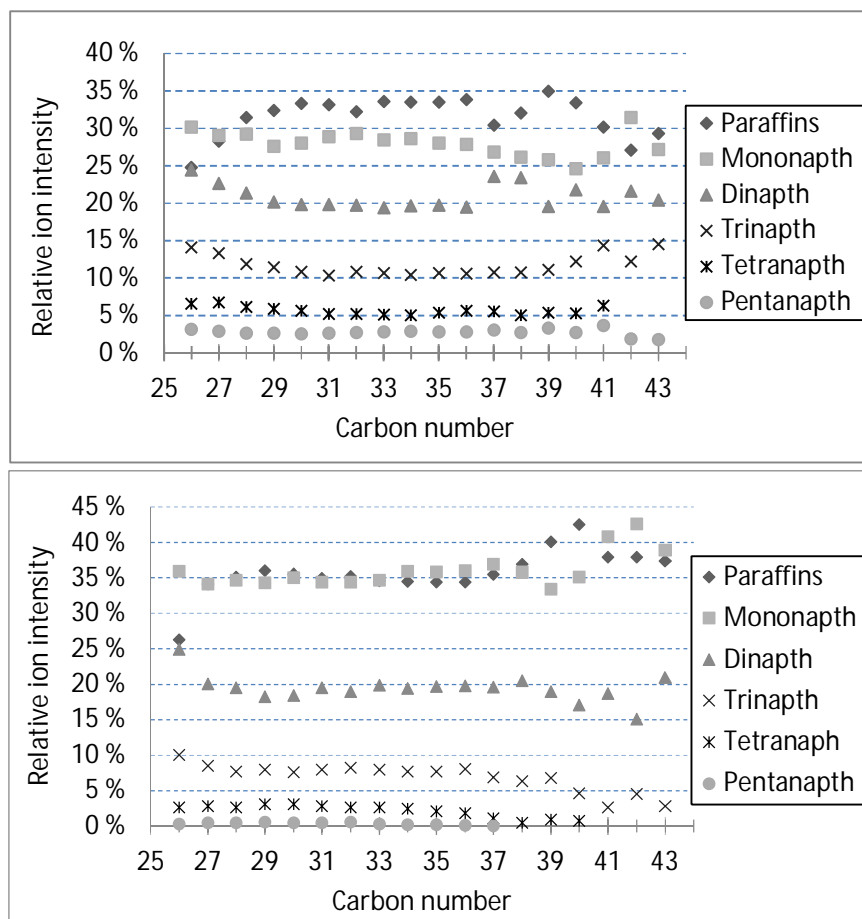




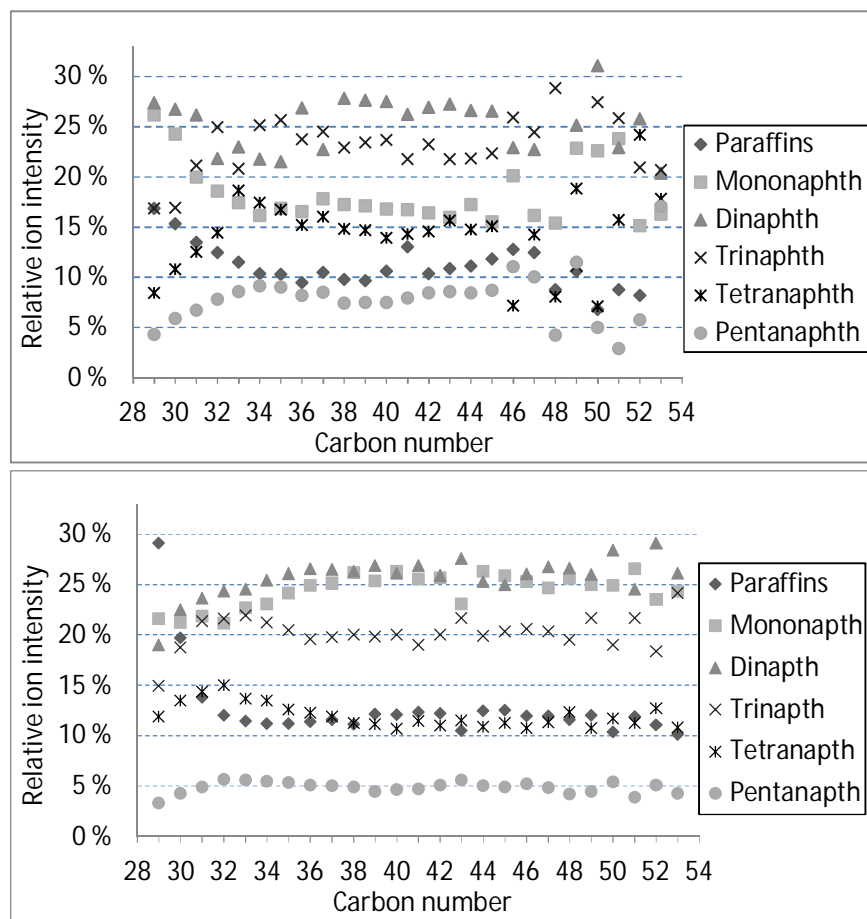
**Figure S7.** Positive ion mode FI mass spectrum of squalane (MW 422) determined using a brand new FI emitter. Zoomed view on the mass spectrum on the left corner shows the fragment ions and  $^{13}\text{C}$  isotope ions. Percent number near fragment ion of  $m/z$  420 refers to the abundance of the fragment ion relative to the molecular ion ( $m/z$  422).




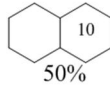
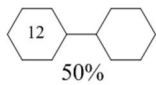
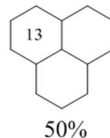
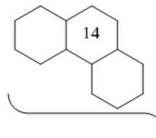
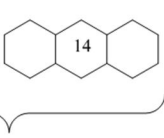
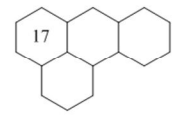
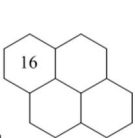
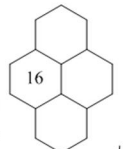
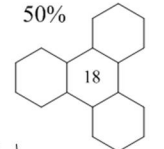
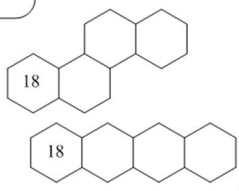
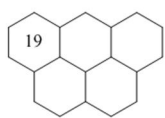
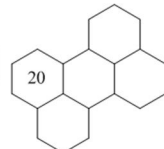
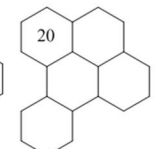
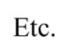



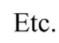
**Figure S8.** Hydrocarbon class distributions as a function of carbon number determined for low viscosity base oil by using APCI-MS (top) and FI-MS (bottom).



**Figure S9.** Hydrocarbon class distributions as a function of carbon number determined for middle viscosity base oil by using APCI-MS (top) and FI-MS (bottom).



**Figure S10.** Hydrocarbon class distributions as a function of carbon number determined for high viscosity base oil by using APCI-MS (top) and FI-MS (bottom).

Hydrocarbon class	AVG number of naphthenic C	
Mononaphthenes	6	
Dinaphthenes	11	 
Trinaphthenes	13.5	   
Tetranaphthenes	17	   
Pentanaphthenes	20	   
Hexanaphthenes		   

**Figure S11.** Naphthenic structures, their total carbon numbers and relative contributions used to calculate average number of naphthenic carbons.